

# Concepts in Monte Carlo sampling

Gabriele Tartero and Werner Krauth\*

*Laboratoire de Physique de l'École normale supérieure,  
ENS, Université PSL, CNRS, Sorbonne Université,  
Université Paris-Diderot, Sorbonne Paris Cité, Paris, France*

(Dated: September 7, 2023)

We discuss modern ideas in Monte Carlo algorithms in the simplified setting of the one-dimensional anharmonic oscillator. After reviewing the connection between molecular dynamics and Monte Carlo, we introduce the Metropolis and the factorized Metropolis algorithms and to lifted non-reversible Markov chains. We furthermore illustrate the concept of thinning, where moves are accepted by simple bounding potentials rather than, in our case, the harmonic and quartic constituents of the anharmonic oscillator. We point out the multiple connections of our example algorithms with real-world sampling problems. The paper is fully self-contained and Python implementations are provided.

## I. INTRODUCTION

The Monte Carlo method is an important tool for producing samples  $x$  from a given probability distribution  $\pi(x)$ . In real-life applications, algorithms and computer implementations for this sampling problem can be highly complex. In this paper, we rather discuss a dozen of distinct Monte Carlo algorithms in the severely stripped-down setting of a particle in a one-dimensional anharmonic potential

$$U_{24}(x) = \frac{x^2}{2} + \frac{x^4}{4} \quad (1)$$

consisting of a harmonic term,  $U_2 = x^2/2$ , and a quartic one,  $U_4 = x^4/4$ . For concreteness, we also provide short example programs.

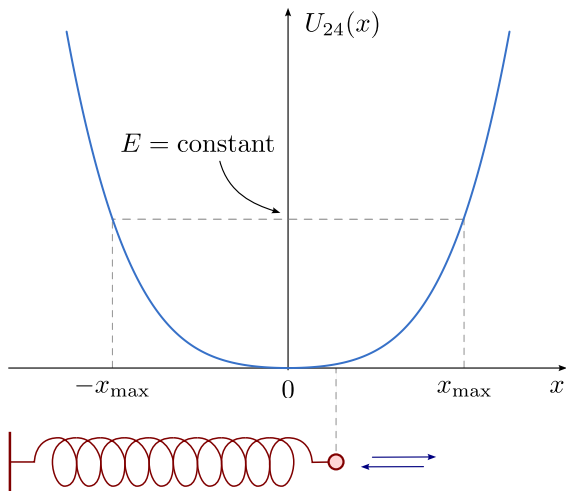


**FIG. 1:** Isolated anharmonic oscillator at energy  $E$ , subject to the potential  $U_{24}$  of Eq. (1).

For the anharmonic oscillator, the distribution to be sampled is the Boltzmann distribution

$$\pi_{24}(x) = \exp[-\beta U_{24}(x)], \quad (2)$$

where  $\beta = (k_B T)^{-1}$  is the inverse of the temperature  $T$ , and  $k_B$  denotes the Boltzmann constant. The connection between the potential  $U_{24}$  and the distribution  $\pi_{24}$  derives from the following. In classical mechanics, an isolated particle is governed by Newton's law and, in a one-dimensional confining potential, oscillates between two turning points. A certain function  $\pi^{\text{iso}}(x)$  describes the fraction of time that the particle spends at position  $x$  during one period and, therefore, during a long time interval containing many periods. If the particle is in contact with a thermostat, this function turns into a probability distribution for finding the particle at a position  $x$  at large times  $t$ , and it is exactly the Boltzmann distribution  $\pi_{24}(x)$  of Eq. (2), as we will discuss (see Sec. II). The molecular-dynamics method generally accesses this distribution through the numerical solution of Newton's equation in contact with a thermostat.

The Monte Carlo method addresses the sampling problem more abstractly than molecular dynamics, as it samples (obtains samples  $x$  from) the distribution  $\pi_{24}(x)$  without simulating a physical process. The sequence of twelve short yet intricate Monte Carlo algorithms that we present here will lead us from the beginning of the method, namely direct sampling and the reversible Metropolis algorithm and its extensions (Sec. III), to non-reversible Markov-chain algorithms (Sec. IV) and to advanced approaches that sample the target distribution with a minimum of evaluations of the potential (Sec. V). Some mathematical results are collected separately (App. A). Our algorithms are presented in compact pseudo-code (as in [1]) and implemented in short, openly accessible, Python programs (App. B). Their correctness is tested to high precision (App. C). A companion paper [2] will translate the concepts discussed here to real-life settings and address efficiency questions whereas in the present paper, we are only concerned with the correctness of the sampling algorithms.

\* [werner.krauth@ens.fr](mailto:werner.krauth@ens.fr)

## II. FROM CLASSICAL TO STATISTICAL MECHANICS

If isolated from the environment, so that the energy is conserved, the anharmonic oscillator of Fig. 1 is a classical, periodic, one-dimensional deterministic system, and we may track the fraction of time per period that the particle spends near a given position  $x$  (Sec. II A). When interacting with a heatbath (for which we suppose a concrete realization), the motion is piecewise deterministic [3], yet random. In this case, we may sample the Boltzmann distribution  $\pi_{24}$  through a molecular-dynamics modeling of the particle subject to Newton's laws and interacting with the thermostat (Sec. II B). At the end of this section, we provide a Monte Carlo algorithm that directly samples  $x$  from the Boltzmann distribution (Sec. II C).

### A. The isolated anharmonic oscillator

We may hold the particle fixed—with velocity  $v = 0$ —then release it at time  $t = 0$  from a position  $x_{\max} > 0$ . If it is isolated, the anharmonic oscillator conserves its energy  $E$ , given by the sum of the kinetic and potential energies at all times  $t \geq 0$ . It thus picks up velocity until it reaches the minimum of the potential at  $x = 0$ , then slows down and turns around at  $-x_{\max}$ , where  $E$  equals the potential energy and the velocity again vanishes (see Fig. 2a). The energy  $E$  is then

$$E = \frac{x_{\max}^2}{2} + \frac{x_{\max}^4}{4} \Leftrightarrow x_{\max} = \sqrt{-1 + \sqrt{1 + 4E}}, \quad (3)$$

as follows from solving a quadratic equation and taking a square root. In between the turning points  $-x_{\max}$  and  $x_{\max}$  the kinetic energy  $\frac{1}{2}(dx/dt)^2$  is positive, and the conservation of energy can be written as

$$E = \frac{1}{2} \left( \frac{dx}{dt} \right)^2 + U_{24}(x) \Leftrightarrow \frac{dx}{dt} = \pm \sqrt{2[E - U_{24}(x)]}, \quad (4)$$

which gives

$$dt = \pm \sqrt{\frac{1}{2[E - U_{24}(x)]}} dx. \quad (5)$$

The period  $\tau$  of the motion, i.e. the time between two realizations of a given position and velocity, corresponds to four times the interval from  $x = 0$  to  $x_{\max}$ ,

$$\begin{aligned} \tau &= 4 \int_0^{x_{\max}} dt = 4 \int_0^{\sqrt{-1 + \sqrt{1 + 4E}}} \frac{1}{\sqrt{2[E - U_{24}(x)]}} dx \\ &= 4 \sqrt{\frac{2}{1 + \sqrt{1 + 4E}}} K \left( \frac{1 - \sqrt{1 + 4E}}{1 + \sqrt{1 + 4E}} \right), \end{aligned} \quad (6)$$

where  $K$  is the complete elliptic integral of the first kind (see Fig. 3). For small  $E$ , the period  $\tau$  agrees with that of

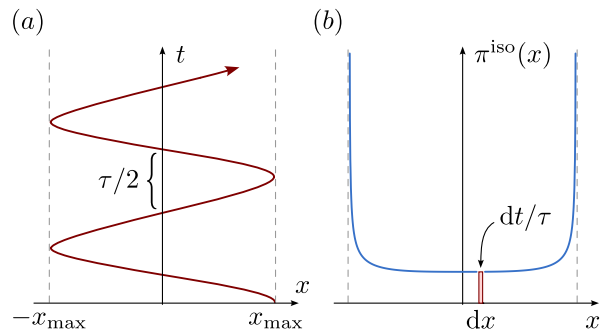


**FIG. 2:** Isolated anharmonic oscillator, as represented in Fig. 1. (a): Periodic trajectory with amplitude  $2x_{\max}$  and period  $\tau$ . (b): Normalized function  $\pi^{\text{iso}}$ . The fraction of time  $dt/\tau$  spent per period between  $x$  and  $x + dx$  is  $\pi^{\text{iso}}(x)dx$ .

the harmonic oscillator, which is famously independent of  $x_{\max}$ , thus of  $E$ . For large  $E$ , in contrast, the period  $\tau \sim E^{-1/4}$  approaches that of the quartic oscillator (see App. A for some mathematical details).

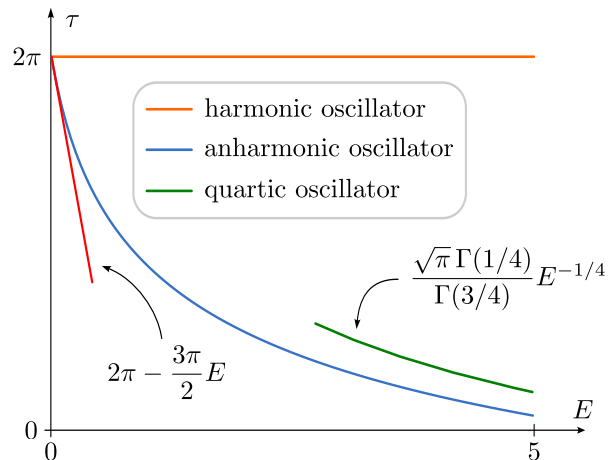


**FIG. 3:** Period  $\tau$  of the isolated anharmonic oscillator as a function of the energy  $E$ . The period of the harmonic oscillator is independent of  $E$ , while that of the quartic oscillator scales as  $E^{-1/4}$ . Here,  $\Gamma$  denotes the Euler gamma function (see App. A).

Equation (5) yields the fraction  $\pi^{\text{iso}}(x)$  of time that the particle spends between  $x$  and  $x + dx$  over a semi-period,

$$\pi^{\text{iso}}(x) = \frac{2}{\tau} \sqrt{\frac{1}{2[E - U_{24}(x)]}}, \quad (7)$$

with  $-x_{\max} < x < x_{\max}$ . The function  $\pi^{\text{iso}}(x)$  is normalized, but it does not represent the probability for the particle to be at  $x$  at a fixed time  $t$ , because of the deterministic nature of the motion (see Fig. 2b).

To simulate the isolated anharmonic oscillator, we could numerically integrate the first-order ordinary differential equation on the right of Eq. (4) over a quarter period and then piece together the entire trajectory

of Fig. 2a. However, this method is specific to one-dimensional dynamical systems [4, §11]. In order to reflect the general case, we numerically integrate Newton’s law for the force  $F$ :

$$F = m \frac{d^2}{dx^2} x(t), \quad \text{with } F = -\frac{dU_{24}}{dx} = -x - x^3. \quad (8)$$

Substituting the time differential  $dt$  by a very small finite interval  $\Delta t$ , appropriate for stepping through, from  $t$  to  $t + \Delta t$ , and to  $t + 2\Delta t$ , and so on, we obtain

$$x(t + \Delta t) = x(t) + v(t)\Delta t, \quad (9)$$

$$v(t + \Delta t) = v(t) - (x + x^3)\Delta t. \quad (10)$$

Alg. 0 (isolated-dynamics) implements one iteration of this naive algorithm, that we set off with an initial position  $x(t = 0) = x_{\max}$ , and an initial velocity  $v(t = 0) = 0$ . The output can then be fed back into the input of the program. As most isolated-molecular-dynamics codes, Alg. 0 is unstable—the energy will slowly increase with time, then diverge. To obtain good approximate results, we should use a small discretization  $\Delta t$  and not run the program up to excessively large values of  $t$ .

```

procedure isolated-dynamics
input  $x, v, t$ 
 $t \leftarrow t + \Delta t$ 
 $x' \leftarrow x + v\Delta t$ 
 $v \leftarrow v - (x + x^3) \Delta t$ 
 $x \leftarrow x'$ 
output  $x, v, t$ 

```

**Algorithm 0:** *isolated-dynamics*. Naive integration of Newton’s equations for the isolated anharmonic oscillator.

## B. Introducing a thermal bath

Liquids, gases and other systems described by statistical mechanics are generally composed of particles that interact and exchange energy and momentum. Any subsystem interacts with its environment and therefore does not conserve energy and momentum. For the anharmonic oscillator, this may be modeled by an external heatbath at temperature  $T$ , represented by a box composed of a very large number of hard-sphere particles of mass  $m = 1$  that fly about randomly with velocities given by the Maxwell distribution. For concreteness, we imagine the anharmonic oscillator to be in contact with the heatbath through a semi-permeable elastic “thermostat”, a stick that vibrates back and forth in an infinitesimal interval around  $x = 0$ , and that is also of mass one. At each collision of the thermostat with a heatbath particle, their two velocities are exchanged. We may imagine that the anharmonic oscillator, as it approaches  $x = 0$ , passes through the thermostat without interaction with probability  $1/2$ , and otherwise bounces off with the velocity

of the stick. The particle trajectory is then deterministic except at the origin (see Fig. 4). Statistical mechanics teaches us that, although all the particles in the heatbath are Maxwell-distributed, the thermostat behaves differently. In particular, since the latter lies at a fixed position (up to an infinitesimal interval), its velocity follows the distribution

$$\pi(v)dv = \beta|v|e^{-\beta v^2/2}dv, \quad (11)$$

often called the Maxwell boundary condition (see [1, Sec. 2.3.1]). It differs by the prefactor  $\beta|v|$  from the Maxwell distribution of one velocity component.

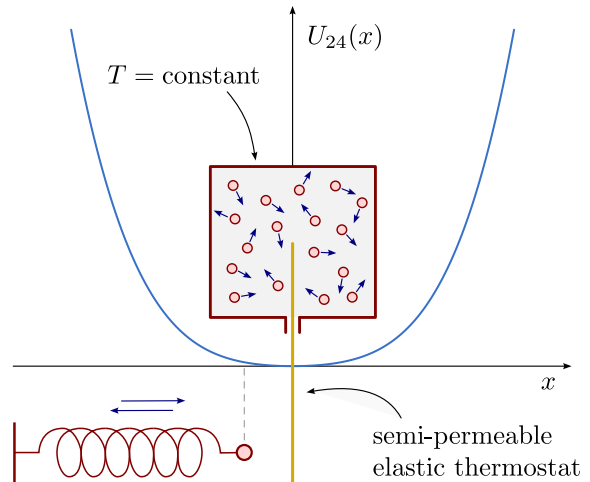


**FIG. 4:** Anharmonic oscillator of Eq. (1) interacting with a heatbath at temperature  $T$  through an elastic semi-permeable thermostat vibrating in an infinitesimal interval about  $x = 0$ .

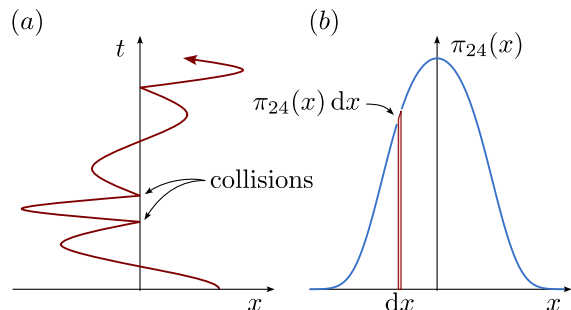


**FIG. 5:** Anharmonic oscillator in contact with the thermostat of Fig. 4. (a): Piecewise deterministic trajectory with random kicks at  $x = 0$ . (b): At large  $t$ , when the initial configuration  $x(t = 0)$  is forgotten, the particle position follows the Boltzmann distribution  $\pi_{24}$  of Eq. (2).

The velocity distribution of the thermostat in Eq. (11) can be sampled as

$$v = \pm \sqrt{\frac{-2 \log \text{ran}(0, 1)}{\beta}}, \quad (12)$$

and the Maxwell boundary condition, thus realized with a single random number, exactly represents the infinite heatbath of Fig. 4. After a few collisions (see Fig. 5a), the particle has forgotten its initial position  $x(0)$ , and it makes sense to speak of the probability distribution at time  $t$ . Exactly given by  $\pi_{24}(x)$  in the limit  $\Delta t \rightarrow 0$ , it substantially differs from  $\pi^{\text{iso}}$  of Fig. 2b and is naively sampled by Alg. 1 (thermostat-dynamics).

```

procedure thermostat-dynamics
input  $x, v, t$ 
 $x' \leftarrow x + v\Delta t$ 
 $t \leftarrow t + \Delta t$ 
 $\Upsilon \leftarrow \text{ran}(0, 1)$ 
if  $xx' < 0$  and  $\Upsilon < 1/2$ :
   $\{ v \leftarrow -\text{sign}(v)\sqrt{-2\beta^{-1} \log \text{ran}(0, 1)}$  (see Eq. (12))
else:
   $\{ v \leftarrow v - (x + x^3)\Delta t$ 
   $\{ x \leftarrow x'$ 
output  $x, v, t$ 

```

**Algorithm 1: thermostat-dynamics.** Naive solution of Newton’s equations for the anharmonic oscillator with the semi-permeable thermostat at  $x = 0$  (see Fig. 4).

We pause for a moment to compute the normalization  $Z(\beta)$  of  $\pi_{24}$  in Eq. (2), that is, the partition function

$$Z(\beta) = \int_{-\infty}^{\infty} dx \pi_{24}(x) = \frac{e^{\beta/8}}{\sqrt{2}} K_{1/4}(\beta/8), \quad (13)$$

where  $K_{1/4}$  denotes the Bessel function of the second kind (see App. A). For simplicity of notation, the division by the partition function is understood whenever we want  $\pi_{24}$  to represent a *bona fide* normalized probability distribution.

### C. Direct Monte Carlo sampling

To sample the distribution  $\pi_{24}$ , one need not simulate a physical system—in our case the anharmonic oscillator in contact with a heatbath. Let us first consider the simpler problem of the Gaussian distribution:

$$\pi_2(x) = \exp[-\beta U_2(x)] = \exp(-\beta x^2/2). \quad (14)$$

Samples  $x$  of  $\pi_2(x)$  are known as Gaussian random numbers of zero mean and of standard deviation  $1/\sqrt{\beta}$ . They are readily available on computers, websites, and even pocket calculators (see [1, Sec. 1.2.5] for an algorithm using the method of sample transformation from uniform random numbers). With an additional uniform random number  $y = \text{ran}[0, \exp(-\beta x^2/2)]$ , they can be expanded into two-dimensional positions  $(x, y)$  of “pebbles” which are uniformly distributed in the area between the  $x$ -axis and the bell-shaped Gaussian curve of Eq. (14).

The distribution of the anharmonic oscillator satisfies  $\pi_{24}(x) \leq \pi_2(x)$  for all  $x$  (see Fig. 6), and it plays

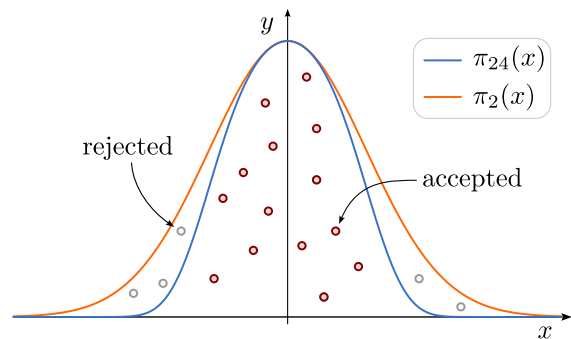


**FIG. 6:** Uniformly distributed pebbles below the Gauss curve  $\pi_2$ . The  $x$ -values of the pebbles  $(x, y)$ , with  $y < \pi_{24}(x)$ , sample the Boltzmann distribution  $\pi_{24}$  of Eq. (2).

no role that it may not be normalized. Those pebbles that lie below  $\pi_{24}$ —as they are uniformly distributed below the Gauss curve—are also evenly spread out below  $\pi_{24}$ . Clearly, it suffices to reject any pebble  $(x, y)$  above  $\pi_{24}$ , to be left with  $x$  positions distributed according to the Boltzmann distribution of the anharmonic oscillator. Algorithm 2 (direct-sampling) implements this direct-sampling idea.

```

procedure direct-sampling
while True:
   $\{ x \leftarrow \text{gauss}(0, 1/\sqrt{\beta})$ 
   $\{ y \leftarrow \text{ran}[0, \pi_2(x)]$ 
  if  $y < \pi_{24}(x)$ : break
output  $x$ 

```

**Algorithm 2: direct-sampling.** Sampling  $\pi_{24}$  through the rejection of Gaussians samples from Eq. (14).

## III. REVERSIBLE MARKOV CHAINS

The probability of rejecting a pebble in Alg. 2 (direct-sampling) is not too high, and a sample of  $\pi_{24}$  is obtained in a split second from a sample of  $\pi_2$ . In real life, however, the difference between any distribution that we can sample (as  $\pi_2$ ) and the one we want to sample (as  $\pi_{24}$ ) becomes huge, thwarting the direct-sampling approach. In the alternative Markov-chain sampling, one starts at time  $t = 0$  with a sample  $x_0$  from a distribution  $\pi^{\{0\}}$  that one knows how to sample. At the next step, the position  $x_1$  samples a distribution  $\pi^{\{1\}}$ , and so on. Introducing the transition matrix  $P$  such that  $P(x', x)$  represents the probability to move from a sample  $x'$  to a sample  $x$  in one time step, the distribution at time  $t + 1$  can be expressed as

$$\pi^{\{t+1\}}(x) = \sum_{x' \in \Omega} \pi^{\{t\}}(x') P(x', x) \quad \forall x \in \Omega, \quad (15)$$

where the sample space  $\Omega$  represents the set of all configurations of the system. Markov-chain Monte Carlo

requires that, at large  $t$ ,  $x_t$  samples the distribution  $\pi^{\{t \rightarrow \infty\}} = \pi$ . For this to take place, the transition matrix  $P$  must satisfy, for all  $x \in \Omega$ , the global-balance condition,

$$\pi(x) = \sum_{x' \in \Omega} \pi(x')P(x', x) \quad (\text{global balance}), \quad (16)$$

which is nothing but the steady-state version of Eq. (15). The strategy for sampling  $\pi$  implied in Eqs. (15) and (16) represents a monumental investment, as we have to wait a long time until  $\pi^{\{t\}} \sim \pi$  in order to get a single sample of  $\pi$ . It is not uncommon for this mixing time to correspond to weeks or even years of computer time [5].

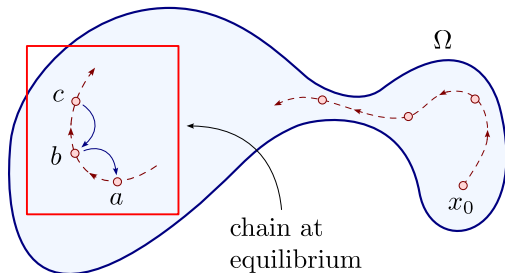


**FIG. 7:** Reversible Markov chain. In equilibrium, it satisfies  $\mathbb{P}(a \rightarrow b \rightarrow c) = \mathbb{P}(c \rightarrow b \rightarrow a)$  for all  $a, b, c \in \Omega$ .

The algorithms in this section are more restrictive than required by Eq. (16). They satisfy, for all  $x, x' \in \Omega$ , the detailed-balance condition:

$$\pi(x)P(x, x') = \pi(x')P(x', x) \quad (\text{detailed balance}). \quad (17)$$

It suffices to sum Eq. (17) over all  $x' \in \Omega$  (using the conservation of probabilities  $\sum_{x'} P(x, x') = 1$ ), in order to see that detailed balance implies global balance.

Detailed-balance algorithms are time-reversible. This means that, at large  $t$  (in equilibrium), any segment of the chain (for example  $[a \rightarrow b \rightarrow c]$  in Fig. 7) at subsequent time steps is sampled with the same probability  $\mathbb{P}$  as the time-reversed segment. In our example,  $\mathbb{P}(a \rightarrow b \rightarrow c)$  is pieced together from the probability  $\pi(a)$  to sample  $a$  and the transition-matrix probabilities to move from  $a$  to  $b$  and then from  $b$  to  $c$ , so that

$$\begin{aligned} \mathbb{P}(a \rightarrow b \rightarrow c) &= \underbrace{\pi(a)P(a, b)}_{\pi(b)P(b, a) \text{ etc.}} P(b, c) \\ &= \pi(c)P(c, b)P(b, a) = \mathbb{P}(c \rightarrow b \rightarrow a), \end{aligned} \quad (18)$$

where we have twice used the detailed-balance condition. By construction, reversible algorithms thus have no net flows (the flow  $a \rightarrow b \rightarrow c$  is cancelled by the flow  $c \rightarrow b \rightarrow a$ ), and this points to a very serious restriction imposed by the detailed-balance condition: they can usually only move around  $\Omega$  diffusively, that is, slowly.

In this section, we will first discuss the seminal reversible algorithm due to Metropolis et al. (Sec. III A).

We will then explore a variant of the Metropolis algorithm which introduces a crucial factorization (Sec. III B). We finally discuss the consensus principle at the origin of modern developments (Sec. III C).

### A. The Metropolis chain

To sample the distribution  $\pi_{24}$  with a reversible transition matrix  $P(x, x')$ , we impose the detailed-balance condition  $\pi(x)P(x, x') = \pi(x')P(x', x)$  for any pair  $x$  and  $x'$  in  $\Omega$ . To this end, we may choose

$$\pi(x)P(x, x') \propto \min[\pi(x), \pi(x')] \quad \text{for } x \neq x'. \quad (19)$$

The right-hand side of Eq. (19) is symmetric in  $x$  and  $x'$ , so that the left-hand side must also be symmetric. Therefore, detailed balance is automatically satisfied. Dividing both sides by  $\pi(x)$ , we arrive at the equation famously proposed by Metropolis et al. in 1953:

$$P^{\text{Met}}(x, x') \propto \min\left[1, \frac{\pi(x')}{\pi(x)}\right] \quad \text{for } x \neq x'. \quad (20)$$

Let us discuss the difference between a transition matrix and a filter, in order to render Eq. (20) explicit and get rid of the proportionality sign. Indeed, the move from  $x$  to  $x' \neq x$  proceeds in two steps. It is first proposed with a symmetric *a priori* probability  $\mathcal{A}(x, x')$  and then is accepted or rejected with a filter:

$$P^{\text{Met}}(x, x') = \underbrace{\mathcal{A}(x, x')}_{\text{transition matrix}} \underbrace{\overbrace{\mathcal{P}^{\text{Met}}(x, x')}}_{\text{Metropolis filter}}.$$

For the Metropolis algorithm, a proposed move  $x \rightarrow x'$  (with  $x' \neq x$ ) is thus accepted with probability

$$P^{\text{Met}}(x, x') = \min\left[1, \frac{\pi(x')}{\pi(x)}\right]. \quad (21)$$

If the move  $x \rightarrow x'$  is rejected, the particle remains at  $x$ . This sets the diagonal transition matrix elements  $P(x, x)$  and guarantees that  $\sum_{x'} P(x, x') = 1$ .

Algorithm 3 (**metropolis**) implements the symmetric *a priori* probability as a uniform displacement  $\Delta = x' - x$  which is as likely as  $-\Delta$ . The Metropolis filter is implemented with a uniform random number  $\Upsilon$  between 0 and 1, that we refer to as a “pebble”. For large times  $t$ , when the initial configuration is forgotten, the algorithm samples  $\pi_{24}$ . In all the following Markov-chain algorithm, this large- $t$  condition is silently understood.

### B. Factorizing the Metropolis filter

The Metropolis algorithm is really famous, but it is not the end of history. A modern variant is useful for

**procedure metropolis**  
**input**  $x$  (sample at time  $t$ )  
 $\Delta \leftarrow \text{ran}(-\delta, \delta)$   
 $x' \leftarrow x + \Delta$   
 $\Upsilon \leftarrow \text{ran}(0, 1)$   
**if**  $\Upsilon < \min \left[ 1, \frac{\pi_{24}(x')}{\pi_{24}(x)} \right]$ :  $x \leftarrow x'$   
**output**  $x$  (sample at time  $t + 1$ )

**Algorithm 3: metropolis.** Sampling  $\pi_{24}$  with the Metropolis algorithm.

distributions  $\pi$  that factorize:

$$\pi = \pi_a \pi_b \pi_c \cdots \pi_k = \prod_{\xi=a, \dots, k} \pi_\xi. \quad (22)$$

For example, the Boltzmann distribution  $\pi = \exp(-\beta U)$  takes the above form if its potential  $U$  can be written as the sum over pair potentials. The Metropolis filter of Eq. (21) is then

$$\begin{aligned} \mathcal{P}^{\text{Met}}(x, x') &= \min \left[ 1, \frac{\pi_a(x') \pi_b(x') \cdots \pi_k(x')}{\pi_a(x) \pi_b(x) \cdots \pi_k(x)} \right] \\ &= \min \left[ 1, \prod_{\xi=a, \dots, k} \frac{\pi_\xi(x')}{\pi_\xi(x)} \right], \end{aligned} \quad (23)$$

and it is implemented in this way in countless computer programs. An alternative to Eq. (23) is the factorized Metropolis filter [6],

$$\begin{aligned} \mathcal{P}^{\text{fact}}(x, x') &= \min \left[ 1, \frac{\pi_a(x')}{\pi_a(x)} \right] \cdots \min \left[ 1, \frac{\pi_k(x')}{\pi_k(x)} \right] \\ &= \prod_{\xi=a, \dots, k} \min \left[ 1, \frac{\pi_\xi(x')}{\pi_\xi(x)} \right]. \end{aligned} \quad (24)$$

If used naively, it gives lower acceptance probabilities than the Metropolis filter, but it also satisfies the detailed-balance condition. Let us prove this for the anharmonic oscillator, where

$$\mathcal{P}_{24}^{\text{fact}}(x, x') = \min \left[ 1, \frac{\pi_2(x')}{\pi_2(x)} \right] \min \left[ 1, \frac{\pi_4(x')}{\pi_4(x)} \right], \quad (25)$$

and where

$$\begin{aligned} \underline{\pi_{24}}(x) &= \exp \left( -\frac{x^2}{2} - \frac{x^4}{4} \right) = \\ &= \exp \left( -\frac{x^2}{2} \right) \exp \left( -\frac{x^4}{4} \right) = \underline{\pi_2}(x) \underline{\pi_4}(x), \end{aligned} \quad (26)$$

illustrating that a potential that is a sum of terms yields a Boltzmann distribution that factorizes. Detailed balance

is satisfied because of the following:

$$\begin{aligned} &\frac{\pi_{24}(x) \mathcal{P}_{24}^{\text{fact}}(x, x')}{\pi_{24}(x') \mathcal{P}_{24}^{\text{fact}}(x', x)} \\ &\propto \underbrace{\pi_2(x) \min \left[ 1, \frac{\pi_2(x')}{\pi_2(x)} \right]}_{\min[\pi_2(x), \pi_2(x')]: x \leftrightarrow x'} \underbrace{\pi_4(x) \min \left[ 1, \frac{\pi_4(x')}{\pi_4(x)} \right]}_{\min[\pi_4(x), \pi_4(x')]: x \leftrightarrow x'} \\ &\quad \times \pi_{24}(x') \mathcal{P}_{24}^{\text{fact}}(x', x), \end{aligned} \quad (27)$$

where we have dropped the symmetric *a priori* probability  $\mathcal{A}$ . Algorithm 4 (**factor-metropolis**) samples  $\pi_{24}$ . It implements the factorized filter in a way that we will soon discover to be naive.

**procedure factor-metropolis**  
**input**  $x$   
 $\Delta \leftarrow \text{ran}(-\delta, \delta)$   
 $x' \leftarrow x + \Delta$   
 $\Upsilon \leftarrow \text{ran}(0, 1)$   
**if**  $\Upsilon < \min \left[ 1, \frac{\pi_2(x')}{\pi_2(x)} \right] \min \left[ 1, \frac{\pi_4(x')}{\pi_4(x)} \right]$ :  
 $\{ x \leftarrow x' \}$   
**output**  $x$

**Algorithm 4: factor-metropolis.** Sampling  $\pi_{24}$  naively with the factorized Metropolis filter.

### C. The consensus principle

The factorized Metropolis algorithm will turn out to be particularly powerful, in the presence of many factors, even an infinite number of them. This is because of the consensus principle, that we now discuss, and which, in the end, will avoid the evaluation of the lengthy product in Eq. (24). For the anharmonic oscillator, the consensus

	Quartic	Accept ( $p_4$ )	Reject ( $1 - p_4$ )
Harmonic			
Accept ( $p_2$ )		$p_2 p_4$ ✓	$p_2(1 - p_4)$
Reject ( $1 - p_2$ )		$(1 - p_2)p_4$	$(1 - p_2)(1 - p_4)$

**TABLE I:** Consensus principle in the factorized Metropolis filter. A move  $x \rightarrow x'$  that is accepted/rejected independently by the harmonic and the quartic factor with probabilities taken from Eq. (28). The acceptance “by consensus” reproduces the correct probability of Eq. (25).

principle simply relies on the fact that the filter

$$\mathcal{P}_{24}^{\text{fact}}(x, x') = \underbrace{\min \left[ 1, \frac{\pi_2(x')}{\pi_2(x)} \right]}_{p_2 \text{ (in Table I)}} \underbrace{\min \left[ 1, \frac{\pi_4(x')}{\pi_4(x)} \right]}_{p_4 \text{ (in Table I)}} \quad (28)$$

is a product  $p_2 p_4$  of probabilities that may be interpreted as independent (see Table I). This holds although the two factors are evidently correlated and,

for example,  $\pi_2$  is small when  $\pi_4$  is. In Alg. 5 (`factor-metropolis(patch)`), two independent decisions are taken, one for the harmonic and one for the quartic factor, and the proposed move is finally accepted only if it is accepted by both factors. The output is identical to that of Alg. 4 (`factor-metropolis`), and it again samples the Boltzmann distribution  $\pi_{24}$ .

```

procedure factor-metropolis(patch)
input  $x$ 
 $\Delta \leftarrow \text{ran}(-\delta, \delta)$ 
 $x' \leftarrow x + \Delta$ 
 $\Upsilon_2 \leftarrow \text{ran}(0, 1)$ ;  $\Upsilon_4 \leftarrow \text{ran}(0, 1)$ 
if  $\Upsilon_2 < \min \left[ 1, \frac{\pi_2(x')}{\pi_2(x)} \right]$  and  $\Upsilon_4 < \min \left[ 1, \frac{\pi_4(x')}{\pi_4(x)} \right]$ :
    {  $x \leftarrow x'$  (move accepted by consensus) }
output  $x$ 

```

**Algorithm 5:** `factor-metropolis(patch)`. Patch of Alg. 4, implementing the consensus principle.

#### IV. GOING BEYOND REVERSIBILITY

In a tradition that started with the Metropolis algorithm, many decades ago, Markov chains are normally designed with the quite restrictive detailed-balance condition, although they are only required to satisfy global balance. In this section, we illustrate modern attempts to overcome the detailed-balance condition in a systematic way, within the framework of “lifted” Markov chains [7, 8]. Our first lifted Markov chain, Alg. 6 (`lifted-metropolis`), holds in fewer than a dozen lines of code, but is quite intricate (Sec. IV A). In recent applications, lifted Markov chains are often formulated for continuous time. For the anharmonic oscillator, this gives the “zig-zag” algorithm [9], where the particle moves back and forth as in molecular dynamics (as in Alg. 0 (`isolated-dynamics`)), but at fixed velocity. Newton’s equations are not solved, but  $\pi_{24}$  is still sampled exactly, and quite magically so (Sec. IV B). The decision to reverse the velocity (from “zig” to “zag”) may again be broken up into independent decisions of the harmonic and the quartic factors foreshadowing strategies that have profoundly impacted real-life sampling approaches (Sec. IV C).

##### A. Lifting the Metropolis chain

The Metropolis algorithm, from a position  $x$ , proposes positive and negative displacements  $\Delta$  for the anharmonic oscillator with symmetric *a priori* probabilities (see Alg. 3 (`metropolis`)). The filter then imposes that the net flow vanishes, so there will be as many particles

to go from  $x$  to  $x + \Delta$  as in the reverse direction, even if, say,  $\pi(x) \ll \pi(x + \Delta)$ .

We will now break detailed balance with a non-reversible “lifted” Markov chain [7, 8] that only respects global balance, while having  $\pi_{24}$  as its stationary distribution. Let us suppose, in a first step, that the positions  $x$  lie on the grid  $\{\dots, -2\Delta, -\Delta, 0, \Delta, 2\Delta, \dots\}$ , with moves allowed only between nearest neighbors. Each configuration  $x$  is duplicated (“lifted”) into two configurations, a forward-moving one  $\{x, +1\}$ , and a backward-moving one  $\{x, -1\}$ . From a lifted configuration  $\{x, \sigma\}$ , the lifted Metropolis algorithm only proposes a forward move if  $\sigma = 1$ , and only a backward move if  $\sigma = -1$ . In summary,

$$P^{\text{lift}}(\{x, \sigma\}, \{x + \sigma\Delta, \sigma\}) = \min \left[ 1, \frac{\pi_{24}(x + \sigma\Delta)}{\pi_{24}(x)} \right],$$

where  $\sigma = \pm 1$ . When this move is not accepted by the Metropolis filter, the algorithm flips the direction and instead moves from  $\{x, \sigma\}$  to  $\{x, -\sigma\}$ :

$$P^{\text{lift}}(\{x, \sigma\}, \{x, -\sigma\}) = 1 - \min \left[ 1, \frac{\pi_{24}(x + \sigma\Delta)}{\pi_{24}(x)} \right]. \quad (29)$$

This algorithm clearly violates detailed balance as, for example,

$$\begin{aligned} P^{\text{lift}}(\{x, +1\}, \{x + \Delta, +1\}) &> 0, \\ P^{\text{lift}}(\{x + \Delta, +1\}, \{x, +1\}) &= 0. \end{aligned}$$

There is thus no backward flow for  $\sigma = +1$  and no forward flow for  $\sigma = -1$ . On the other hand, the lifted Metropolis algorithm satisfies the global-balance condition of Eq. (16) with the “ansatz”

$$\pi_{24}^{\text{lift}}(\{x, \sigma\}) = \frac{1}{2} \pi_{24}(x) \quad \text{for } \sigma = \pm 1. \quad (30)$$

For example, the flow into the lifted configuration  $\{x, +1\}$  satisfies

$$\begin{aligned} \pi_{24}(\{x, +1\}) = & \\ & \pi_{24}(\{x - \Delta, +1\}) P^{\text{lift}}(\{x - \Delta, +1\}, \{x, +1\}) \\ & + \pi_{24}(\{x, -1\}) P^{\text{lift}}(\{x, -1\}, \{x, +1\}). \end{aligned} \quad (31)$$

The two contributions on the right-hand side of eq. (31) correspond on the one hand to the accepted moves from  $\{x - \Delta, +1\}$ , and on the other hand to the lifted moves from  $\{x, -1\}$ , when the move from  $\{x, -1\}$  towards  $\{x - \Delta, -1\}$  is rejected (see Fig. 8). Equation (31) can be transformed into

$$\begin{aligned} \pi_{24}(x) = \pi_{24}(x - \Delta) \min \left[ 1, \frac{\pi_{24}(x)}{\pi_{24}(x - \Delta)} \right] + \\ \pi_{24}(x) \left\{ 1 - \min \left[ 1, \frac{\pi_{24}(x - \Delta\sigma)}{\pi_{24}(x)} \right] \right\}, \end{aligned}$$

which is identically satisfied. We have shown that the lifted Metropolis algorithm satisfies the global-balance

condition for the ansatz of eq. (30), which splits  $\pi_{24}(x)$  equally between  $\{x, +1\}$  and  $\{x, -1\}$ . The sequence  $\pi^{t\}$  will actually converge towards this stationary distribution under very mild conditions that are satisfied for the anharmonic oscillator [10, 11].

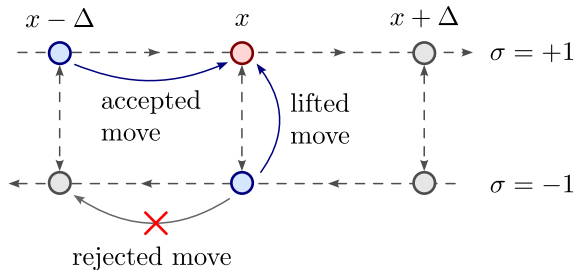


**FIG. 8:** Discretized lifted Metropolis algorithm for the anharmonic oscillator. The flow into the lifted configuration  $\{x, +1\}$  is indicated (see Eq. (31)).

In the lifted Metropolis algorithm, the particle, starting from  $x_0 = 0$ , climbs uphill in direction  $\sigma$  until a move is rejected by the filter, when it remains at its current position but reverses its velocity to  $-\sigma$ . The following downhill moves, again without rejections, are followed by another uphill climb, and so on, criss-crossing between the two wings of the potential  $U_{24}$ . Algorithm 6 (`lifted-metropolis`) implements a version of the lifted Metropolis algorithm where the displacements  $\Delta$  are sampled from a positive interval. The algorithm outputs lifted configurations  $\{x, \sigma\}$  of which, remarkably, the  $x$  positions sample  $\pi_{24}$ .

```

procedure lifted-metropolis
input  $\{x, \sigma\}$  (lifted sample at time  $t$ )
 $\Delta \leftarrow \text{ran}(0, \delta)$  ( $\delta > 0$ )
 $x' \leftarrow x + \sigma\Delta$  ( $x'$  in direction  $\sigma$  from  $x$ )
 $\Upsilon \leftarrow \text{ran}(0, 1)$ 
if  $\Upsilon < \min\left[1, \frac{\pi_{24}(x')}{\pi_{24}(x)}\right]$ :  $x \leftarrow x'$ 
else:  $\sigma \leftarrow -\sigma$ 
output  $\{x, \sigma\}$  (lifted sample at time  $t + 1$ )

```

**Algorithm 6:** `lifted-metropolis`. Non-reversible lifted version of Alg. 3 (`metropolis`). The  $x$ -positions that are output by this program sample  $\pi_{24}$ .

## B. From discrete to continuous time

So far, we have discussed Markov chains that move between configurations indexed by an integer time  $t$ , from  $x_t$  to  $x_{t+1}$ . We now consider algorithms in continuous time (technically speaking, we consider Markov “processes”). For simplicity, we revisit the lifted Metropolis algorithm with its grid of posi-

tions  $\{\dots, -2\Delta, -\Delta, 0, \Delta, 2\Delta, \dots\}$  and with its nearest-neighbor moves, but consider the case of small  $\Delta$ . It is then appropriate to rescale time such that a displacement  $\pm\Delta$  is itself undertaken in a time interval  $\Delta$ . The particle in the anharmonic oscillator thus moves with unit absolute velocity, whose sense is reversed when there is a rejection. The downhill moves are all accepted, and even uphill moves are accepted with a probability close to one. One may sample the position of the next rejection, rather than running through the sequence of individual moves, because an uphill move starting, say, in positive direction from  $x = 0$  is accepted with probability  $\exp[-\beta\Delta U_{24}(x = 0)]$ . Likewise, the probability for accepting a whole sequence of  $n$  uphill moves, at subsequent positions  $0, \Delta, \dots, (n-1)\Delta$ , and then rejecting the move  $n + 1$ , is

$$\mathbb{P}(0 \rightarrow x_{\text{ev}}) = \underbrace{e^{-\beta\Delta U_{24}(0) \cdots \Delta U_{24}[(n-1)\Delta]}}_{n \text{ accepted moves}} \underbrace{\left[1 - e^{-\beta\Delta U_{24}(n\Delta)}\right]}_{\text{rejection}} \rightarrow \beta e^{-\beta U_{24}} dU_{24}. \quad (32)$$

In the small- $\Delta$  limit, the rejection is here expanded to first order, and  $\Delta U$  is replaced by  $dU$ . In our example of the anharmonic oscillator starting at  $x = 0$ , all the increments of  $\Delta U_{24}$  up to position  $x$  add up to the potential  $U_{24}(x)$ . Equation (32) indicates that the value of  $U_{24}$  at which the velocity is reversed follows an exponential distribution in  $U_{24}$  [12]. As an exponential random number can be obtained as a logarithm of a uniform random number (see [1, Sec. 1.2.4]), this yields

$$U_{24}(x_{\text{ev}}) = -\beta^{-1} \log \text{ran}(0, 1). \quad (33)$$

Inverting  $U_{24}(x_{\text{ev}}) = x_{\text{ev}}^2/2 + x_{\text{ev}}^4/4$ , this results in

$$x_{\text{ev}} = \sigma \sqrt{-1 + \sqrt{1 - 4\beta^{-1} \log \text{ran}(0, 1)}}. \quad (34)$$

To sample the Boltzmann distribution  $\pi_{24}$ , it now suffices to sample the turning points  $x_{\text{ev}}$  of the constant-velocity motion, alternatingly on the negative and positive branches of the potential, and then to sample the particle positions at equal time steps, as implemented in Alg. 7 (`zig-zag`). This event-driven continuous-time algorithm samples the Boltzmann distribution  $\pi_{24}$  (see Fig. 9). The event-driven version of Alg. 6 exists also for fixed, finite  $\Delta$ , and it is often classified as “faster-than-the-clock” (see [1, Sec. 7.1.1]).

## C. Extending the consensus principle

We now replace the Metropolis filter in Alg. 7 (`zig-zag`) (contained in the formula for  $x_{\text{ev}}$ ) by the factorized Metropolis filter, and then use the consensus principle. Starting again at  $x = 0$ , the particle now climbs up one hill for the harmonic factor and one for the quartic factor (see Fig. 10). For each factor, we can redo the



```

procedure zig-zag
input  $\{x, \sigma\}, t$  (lifted sample with  $\sigma x \leq 0$ )
 $x_{\text{ev}} \leftarrow \sigma \sqrt{-1 + \sqrt{1 - 4\beta^{-1} \log \text{ran}(0, 1)}}$  (see Eq. (34))
 $t_{\text{ev}} \leftarrow t + |x_{\text{ev}} - x|$ 
for  $t^* = \text{int}(t) + 1, \dots, \text{int}(t_{\text{ev}})$ :
  { print  $x + \sigma(t^* - t)$  (equal-time samples)
 $x \leftarrow x_{\text{ev}}; \sigma \leftarrow -\sigma; t \leftarrow t_{\text{ev}}$  (“zig-zag”)
output  $\{x, \sigma\}, t$ 

```

**Algorithm 7: zig-zag.** Continuous-time version of Alg. 6 (lifted-metropolis) using an event-driven formulation. The  $x$ -positions output by the **print** statement sample  $\pi_{24}$ .

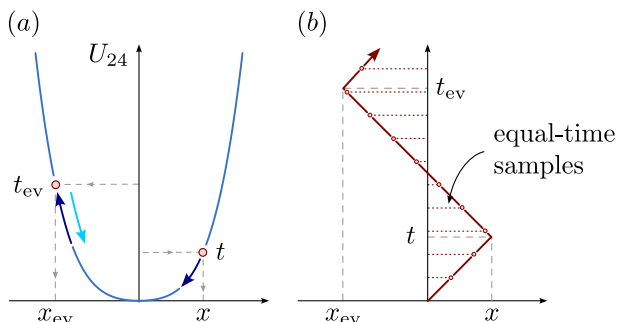


**FIG. 9:** Zig-zag algorithm (continuous-time event-driven lifted Metropolis chain). (a): The particle swings about the origin, turning around at positions  $x_{\text{ev}}$  (sampled by Eq. (34)). (b): Piecewise deterministic constant-velocity trajectory. Particle positions are sampled at equal time steps.

argument of Eq. (32), with  $U_2$  or  $U_4$  instead of  $U_{24}$ . In analogy with eqs. (33) and (34), we can thus sample two “candidate” events,

$$x_{\text{ev}}^{(2)} = \sigma \sqrt{-2\beta^{-1} \log \text{ran}(0, 1)}, \quad (35)$$

$$x_{\text{ev}}^{(4)} = \sigma \sqrt[4]{-4\beta^{-1} \log \text{ran}(0, 1)}, \quad (36)$$

with two independent random numbers. The consensus of the two factors is broken by the candidate event that comes first,

$$x_{\text{ev}} = \sigma \min(|x_{\text{ev}}^{(2)}|, |x_{\text{ev}}^{(4)}|), \quad (37)$$

when the velocity must be reversed. We may again collect positions  $x$  at equal time steps. This is implemented in Alg. 8 (factor-zig-zag), which samples the Boltzmann distribution  $\pi_{24}$ .

## V. THINNING: OR, AVOIDING EVALUATION

In molecular-dynamics algorithms such as Alg. 1, forces must be computed precisely in order to keep the trajectory on track. In contrast, Monte Carlo algorithms

```

procedure factor-zig-zag
input  $\{x, \sigma\}, t$  (lifted sample with  $\sigma x \leq 0$ )
 $x_{\text{ev}}^{(2)} \leftarrow \sigma \sqrt{-2\beta^{-1} \log \text{ran}(0, 1)}$  (see Eq. (35))
 $x_{\text{ev}}^{(4)} \leftarrow \sigma \sqrt[4]{-4\beta^{-1} \log \text{ran}(0, 1)}$  (see Eq. (36))
 $x_{\text{ev}} \leftarrow \sigma \min(|x_{\text{ev}}^{(2)}|, |x_{\text{ev}}^{(4)}|)$ 
 $t_{\text{ev}} \leftarrow t + |x_{\text{ev}} - x|$ 
for  $t^* = \text{int}(t) + 1, \dots, \text{int}(t_{\text{ev}})$ :
  { print  $x + \sigma(t^* - t)$  (sample of  $\pi_{24}$ )
 $x \leftarrow x_{\text{ev}}; \sigma \leftarrow -\sigma; t \leftarrow t_{\text{ev}}$  (“zig-zag”)
output  $\{x, \sigma\}, t$ 

```

**Algorithm 8: factor-zig-zag.** Factorized zig-zag algorithm accepting moves in direction  $\sigma$  until the consensus of the harmonic and the quartic factor is broken at position  $x_{\text{ev}}$ .

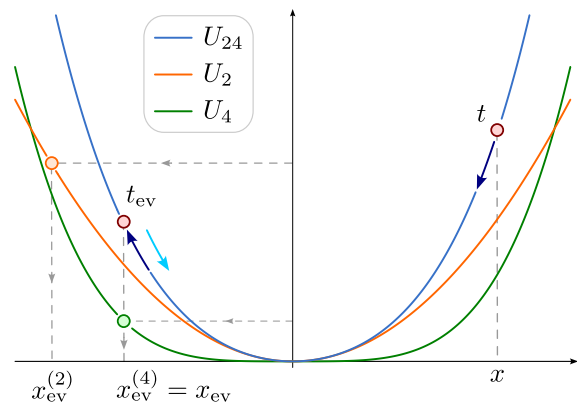


**FIG. 10:** Factorized zig-zag algorithm. Starting from  $x$  (here with  $\sigma = -1$ , the next event is given by the earliest event between  $x_{\text{ev}}^{(2)}$  and  $x_{\text{ev}}^{(4)}$  (here, by  $x_{\text{ev}}^{(4)} = x_{\text{ev}}$ ).

are decision problems where proposed moves must be accepted with a filter, for example the Metropolis filter  $\min[1, \exp(-\beta\Delta U)]$ . As we discuss in this section, one can often base the accept/reject decision on a bounding potential  $\hat{U}$ , and thus avoid computing  $U$ ,  $\Delta U$ , and their exponentials (Sec. VA). In the continuous-time setting, one simply evaluates the derivative of the bounding potential and of the potential  $U$ , in order to eliminate all bias due to the bounding (Sec. VB).

Combining this so-called “thinning” approach [13] with the factorization, we may, in the anharmonic oscillator, base our decision to accept moves on the consensus of harmonic and quartic bounding potentials. At the end, we will set up a Monte Carlo algorithm that evaluates a single factor potential, and only at the position where the proposed move is rejected by the bounding potential of that same factor (Sec. VC). In the companion paper [2], we generalize this approach to real-life simulations of particles with long-range interactions that sample the Boltzmann distribution  $\exp(-\beta U)$  without ever evaluating  $U$ .

### A. Introducing the bounding potential

We say that  $\widehat{U}$  is a bounding potential of a potential  $U$  if, for any pair of configurations  $x$  and  $x'$ , it satisfies

$$\min(1, e^{-\beta\Delta\widehat{U}}) \leq \min(1, e^{-\beta\Delta U}) \quad \forall x, x' \in \Omega, \quad (38)$$

where  $\Delta\widehat{U} = \widehat{U}(x') - \widehat{U}(x)$  and  $\Delta U = U(x') - U(x)$ . This requires  $d\widehat{U}/dx$  and  $dU/dx$  to have the same sign everywhere, with  $|d\widehat{U}/dx| \geq |dU/dx|$ . Concretely, we define the harmonic and quartic bounding potentials as

$$\widehat{U}_2(n) = \begin{cases} 0 & \text{if } n = 0 \\ \widehat{U}_2(|n| - 1) + |n| & \text{if } n \in \mathbb{Z} \setminus \{0\} \end{cases},$$

$$\widehat{U}_4(n) = \begin{cases} 0 & \text{if } n = 0 \\ \widehat{U}_4(|n| - 1) + |n|^3 & \text{if } n \in \mathbb{Z} \setminus \{0\}. \end{cases}$$

These definitions are extended to non-integer arguments  $x$  through linear interpolation. The anharmonic bounding potential is then defined as  $\widehat{U}_{24}(x) = \widehat{U}_2(x) + \widehat{U}_4(x)$  (see Fig. 11).

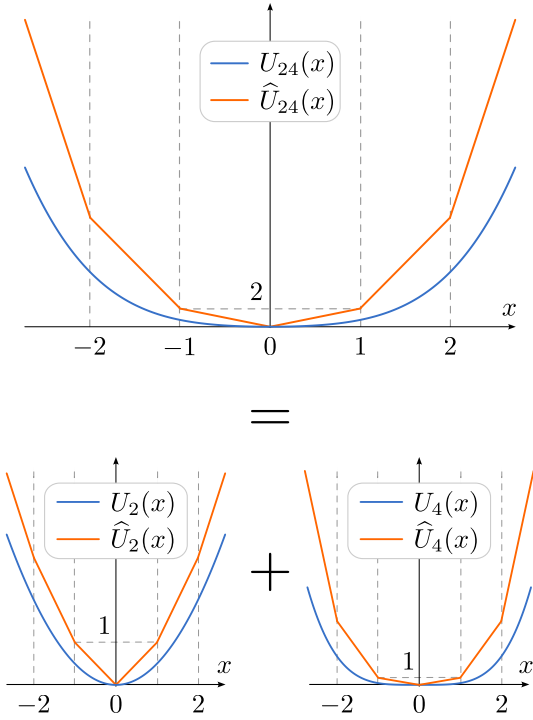


**FIG. 11:** Anharmonic bounding potential  $\widehat{U}_{24}$  and its harmonic and quartic constituents  $\widehat{U}_2$  and  $\widehat{U}_4$ .

A bounding potential can simplify the decision to accept a move as, evidently, a pebble  $0 < \Upsilon < 1$  that falls below  $\exp(-\beta\Delta\widehat{U})$  also falls below  $\exp(-\beta\Delta U)$  (see Fig. 12a). In the remaining algorithms of this paper, we rather use a two-pebble strategy for the decision to accept or reject a move. A first pebble  $0 < \Upsilon_1 < 1$  then decides whether a move is accepted with respect to the

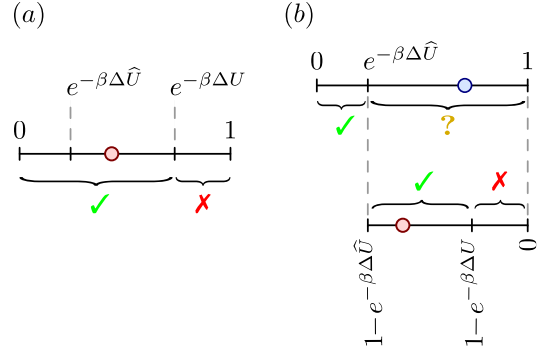


**FIG. 12:** Single-pebble and two-pebble decisions in the Metropolis algorithm. (a): A single pebble  $\Upsilon$  illustrating that acceptance with respect to the bounding potential implies acceptance with respect to  $U$ . (b): A first pebble  $\Upsilon_1$  takes a decision with respect to the bounding potential. In case of rejection, a second pebble  $\Upsilon_2$  definitely decides on the move.

bounding potential. Otherwise (if  $\Upsilon_1$  rejects the move), we use a second pebble  $\Upsilon_2$  to decide whether the first-pebble rejection with respect to  $\widehat{U}$  stands with respect to  $U$  (see Fig. 12b). A rescaling, with  $0 < \Upsilon_2 < 1$ , allows us to definitely reject the move if

$$\Upsilon_2 < \frac{1 - e^{-\beta\Delta U}}{1 - e^{-\beta\Delta\widehat{U}}}. \quad (39)$$

The two-pebble bounding-potential algorithm is implemented in Alg. 9 (bounded-lifted) for the anharmonic oscillator. It again samples the Boltzmann distribution  $\pi_{24}$ .

```

procedure bounded-lifted
input  $\{x, \sigma\}$  (lifted sample at time  $t$ )
 $\Delta \leftarrow \text{ran}(0, \delta)$  ( $\delta > 0$ )
 $x' \leftarrow x + \sigma \Delta$ ;  $\Upsilon_1 \leftarrow \text{ran}(0, 1)$ ;
if  $\Upsilon_1 < \min(1, e^{-\beta\Delta\widehat{U}_{24}})$ :
     $\{ x \leftarrow x'$ 
else:
     $\{ \Upsilon_2 \leftarrow \text{ran}(0, 1)$ 
    if  $\Upsilon_2 > \frac{1 - e^{-\beta\Delta U_{24}}}{1 - e^{-\beta\Delta\widehat{U}_{24}}}$ :  $x \leftarrow x'$ 
    else:  $\sigma \leftarrow -\sigma$ 
output  $\{x, \sigma\}$  (lifted sample at time  $t + 1$ )

```

**Algorithm 9: bounded-lifted.** Discrete-time bounded-lifted Metropolis algorithm using two-pebble decisions. The second pebble is used and the true potential  $U_{24}$  is evaluated only after a first-pebble rejection with respect to the bounding potential  $\widehat{U}_{24}$ .

## B. Continuous-time thinning

The bounded-lifted Metropolis algorithm, Alg. 9 (**bounded-lifted**), generalizes to continuous time. In the anharmonic oscillator, we first consider  $\sigma = +1$  and positive  $x$  between  $n$  and  $n + 1$ , where the decision of Eq. (39), for the second pebble, turns into

$$\Upsilon_2 < \frac{1 - e^{-\beta\Delta U_{24}}}{1 - e^{-\beta\Delta\widehat{U}_{24}}} \rightarrow \Upsilon_2 < \frac{dU_{24}/dx}{d\widehat{U}_{24}/dx}. \quad (40)$$

The piecewise linear anharmonic bounding potential  $\widehat{U}_{24}$  simplifies the event-driven formulation. Rather than to walk up the anharmonic potential until the change of potential satisfies  $\Delta U_{24} = -\beta^{-1} \log \text{ran}(0, 1)$  (see Eq. (33) and Fig. 9), we now run up a bounding potential of constant slope  $\hat{q}$  with

$$\hat{q} = \left. \frac{d}{dx} \widehat{U}_{24}(x) \right|_{x \in S_n} = n + 1 + (n + 1)^3, \quad (41)$$

where  $S_n = [n, n + 1)$  and  $n \in \mathbb{N}$ . The change in potential  $\Delta\widehat{U}_{24}(x) = -\beta^{-1} \log \text{ran}(0, 1)$  then translates into the advance of the position as

$$x_{\text{ev}} = x_0 + (\beta\hat{q})^{-1} \log \text{ran}(0, 1). \quad (42)$$

The event rate  $\beta\hat{q}$  is constant in the sector  $S_n$ , but if  $x_{\text{ev}}$  falls outside of  $S_n$ , it is invalid. In this case, a ‘‘boundary event’’ is triggered, and the particle is placed at the right boundary of  $S_n$ , without changing the direction  $\sigma$ . Otherwise (if  $x_{\text{ev}} \in S_n$ ), the direction  $\sigma$  is reversed if the condition on the pebble  $\Upsilon_2$  in Eq. (40) is satisfied (see Fig. 13).

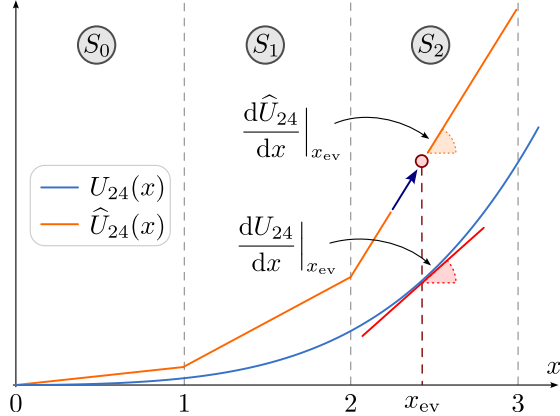


**FIG. 13:** Continuous-time version of the bounded-lifted Metropolis algorithm. The proposed event  $x_{\text{ev}}$  is confirmed by comparing the derivatives of the true potential  $U_{24}$  and the bounding potential  $\widehat{U}_{24}$  (see Eq. (40)).

Our description of the continuous-time bounded-lifted Metropolis algorithm was for the case  $\sigma = 1$ , that is, for a pebble that climbs up the  $x > 0$  branch of the potential. The general case is implemented in Alg. 10 (**bounded-zig-zag**), and it again samples the Boltzmann distribution  $\pi_{24}$ .

## procedure bounded-zig-zag

```

input  $\{x, \sigma\}, t$  (lifted sample)
if  $\sigma x < 0$ :  $x_0 \leftarrow 0$ ; else:  $x_0 \leftarrow x$  (starting point)
 $n \leftarrow \text{int}(|x_0|)$ ;  $\hat{q} \leftarrow n + 1 + (n + 1)^3$ ;  $\tilde{\sigma} \leftarrow \sigma$ 
 $x_{\text{ev}} \leftarrow x_0 + \sigma [-(\beta\hat{q})^{-1} \log \text{ran}(0, 1)]$  (see Eq. (42))
if  $|x_{\text{ev}}| > n + 1$ :
   $\{ x_{\text{ev}} \leftarrow \sigma(n + 1)$ 
else if  $\text{ran}(0, 1) < |x_{\text{ev}} + x_{\text{ev}}^3|/\hat{q}$ :
   $\{ \tilde{\sigma} \leftarrow -\sigma$ 
 $t_{\text{ev}} \leftarrow t + |x_{\text{ev}} - x|$ 
for  $t^* = \text{int}(t) + 1, \dots, \text{int}(t_{\text{ev}})$ :
   $\{ \text{print } x + \sigma(t^* - t)$  (equal-time samples)
 $x \leftarrow x_{\text{ev}}$ ;  $\sigma \leftarrow \tilde{\sigma}$ ;  $t \leftarrow t_{\text{ev}}$  (“zig-zag”)
output  $\{x, \sigma\}, t$ 

```

**Algorithm 10:** **bounded-zig-zag.** Continuous-time bounded-lifted Metropolis algorithm. It need not invert the potential  $U_{24}$  (compare with Eq. (34)), foreshadowing the use of bounding potentials in real-world applications.

## C. Thinning with consensus

Algorithm 10 (**bounded-zig-zag**) avoids the inversion in Eq. (34) of the potential  $U_{24}$ , and only evaluates the derivative  $dU_{24}/dx$  at  $x = \hat{x}_{\text{ev}}$ . At the end of our journey through advanced Markov chain Monte Carlo sampling, we combine the consensus principle underlying factorization with that of thinned, lifted Metropolis chains and sample  $\pi_{24} = \exp(-\beta U_{24})$  without ever evaluating the potential  $U_{24}$  nor its derivative. The use of bounding potentials generalizes to applications in particle systems with long-range interactions. In the anharmonic oscillator, we illustrate the basic idea [14] with the harmonic and quartic factor potentials  $U_2$  and  $U_4$  and their bounding potentials  $\widehat{U}_2$  and  $\widehat{U}_4$ .

With factorization, two candidate events  $x_{\text{ev}}^{(2)}$  and  $x_{\text{ev}}^{(4)}$  can be sampled by means of Eq. (42), with bounding event rates  $\beta(n + 1)$  and  $\beta(n + 1)^3$ , respectively. When both events fall outside the sector  $S_n$  where the bounding rates are valid, a boundary event is triggered. Otherwise, the earliest candidate event  $x_{\text{ev}} \in S_n$  (either  $x_{\text{ev}}^{(2)}$  or  $x_{\text{ev}}^{(4)}$ ) is confirmed with one of the probabilities

$$\frac{dU_2/dx}{d\widehat{U}_2/dx} \Big|_{x_{\text{ev}}=x_{\text{ev}}^{(2)}} = \frac{x_{\text{ev}}}{n + 1}, \quad \frac{dU_4/dx}{d\widehat{U}_4/dx} \Big|_{x_{\text{ev}}=x_{\text{ev}}^{(4)}} = \frac{x_{\text{ev}}^3}{(n + 1)^3}.$$

This bounded-lifted, and in addition factorized, Metropolis algorithm, largely analogous to Alg. 10, is implemented in Alg. 11 (**bounded-factor-zig-zag**). Remarkably, it evaluates the derivative of only one factor potential. Most of the decisional burden is carried by the bounding potentials, for example which factor to choose for the next event. The decision-problem footprint of Monte Carlo algorithms thus appears clearly, as there

are different ways to reach a statistically correct decision. In molecular dynamics, in contrast, only a single Newtonian trajectory exists.

```

procedure bounded-factor-zig-zag
input  $\{x, \sigma\}, t$  (lifted sample at time  $t$ )
if  $\sigma x < 0$ :  $x_0 \leftarrow 0$ ; else:  $x_0 \leftarrow x$  (starting point)
 $n \leftarrow \text{int}(|x_0|)$ ;  $\hat{q}^{(2)} \leftarrow n + 1$ ;  $\hat{q}^{(4)} \leftarrow (n + 1)^3$ ;  $\tilde{\sigma} \leftarrow \sigma$ 
 $x_{\text{ev}}^{(2)} \leftarrow x_0 + \sigma \left[ -(\beta \hat{q}^{(2)})^{-1} \log \text{ran}(0, 1) \right]$  (see Eq. (42))
 $x_{\text{ev}}^{(4)} \leftarrow x_0 + \sigma \left[ -(\beta \hat{q}^{(4)})^{-1} \log \text{ran}(0, 1) \right]$  (see Eq. (42))
if  $\min(|x_{\text{ev}}^{(2)}|, |x_{\text{ev}}^{(4)}|) > n + 1$ :  $x_{\text{ev}} \leftarrow \sigma(n + 1)$ 
else if  $|x_{\text{ev}}^{(2)}| < |x_{\text{ev}}^{(4)}|$ :
   $\left\{ \begin{array}{l} x_{\text{ev}} \leftarrow x_{\text{ev}}^{(2)}; \text{if } \text{ran}(0, 1) < |x_{\text{ev}}|/\hat{q}^{(2)}: \tilde{\sigma} = -\sigma \end{array} \right.$ 
else:
   $\left\{ \begin{array}{l} x_{\text{ev}} \leftarrow x_{\text{ev}}^{(4)}; \text{if } \text{ran}(0, 1) < |x_{\text{ev}}|^3/\hat{q}^{(4)}: \tilde{\sigma} = -\sigma \end{array} \right.$ 
 $t_{\text{ev}} \leftarrow t + |x_{\text{ev}} - x|$ 
for  $t^* = \text{int}(t) + 1, \dots, \text{int}(t_{\text{ev}})$ :
   $\left\{ \begin{array}{l} \text{print } x + \sigma(t^* - t) \quad (\text{equal-time samples}) \end{array} \right.$ 
 $x \leftarrow x_{\text{ev}}; \sigma \leftarrow \tilde{\sigma}; t \leftarrow t_{\text{ev}}$  ("zig-zag")
output  $\{x, \sigma\}, t$ 

```

**Algorithm 11: bounded-factor-zig-zag.** Factorized version of Alg. 10, with one candidate event for each factor (see patch). For each event, only one factor derivative is evaluated.

	Quartic	Accept $(1 - \beta \hat{q}^{(4)} dt)$	Reject $(\beta \hat{q}^{(4)} dt)$
Harmonic			
Accept $(1 - \beta \hat{q}^{(2)} dt)$		$1 - \beta(\hat{q}^{(2)} + \hat{q}^{(4)})dt$	$\beta \hat{q}^{(4)} dt$
Reject $(\beta \hat{q}^{(2)} dt)$		$\beta \hat{q}^{(2)} dt$	0

**TABLE II:** Consensus probabilities of Table I for Alg. 11 (bounded-factor-zig-zag) and its patch. The total event rate (the total rate of rejection by consensus) is the sum of the factor event rates, as terms of order  $(dt)^2$  drop out.

Algorithm 11 (bounded-factor-zig-zag) samples as many candidate events as there are factors (in our case,  $\hat{x}_{\text{ev}}^{(2)}$  and  $\hat{x}_{\text{ev}}^{(4)}$  for the harmonic and quartic factors), thus adopting a strategy that runs into trouble when there are too many factors. A patch of Alg. 11 illustrates, in a nutshell, how factors can be bundled in the continuous-time setting, where the total event rate is the sum of the individual factor rates (see Table II). In the anharmonic oscillator, the total bounding event rate is the sum of the harmonic and the quartic bounding rates, giving us the next event with a single random number. It then remains to decide whether this event is a harmonic-bounding or a quartic-bounding event, as implemented in Alg. 12 (bounded-factor-zig-zag(patch)). Even for a large number of factors, we can take this decision in a few steps, using the famous Walker algorithm [15]. It is this

very program that is used in state-of-the-art programs to handle millions of factors in constant time [14], as we will further discuss in the companion paper [2].

```

procedure bounded-factor-zig-zag(patch)
input  $\{x, \sigma\}, t$  (lifted sample at time  $t$ )
if  $\sigma x < 0$ :  $x_0 \leftarrow 0$ ; else:  $x_0 \leftarrow x$  (starting point)
 $n \leftarrow \text{int}(|x_0|)$ 
 $\hat{q}^{(2)} \leftarrow n + 1$ ;  $\hat{q}^{(4)} \leftarrow (n + 1)^3$ ;  $\hat{q} \leftarrow \hat{q}^{(2)} + \hat{q}^{(4)}$ ;  $\tilde{\sigma} \leftarrow \sigma$ 
 $x_{\text{ev}} \leftarrow x_0 + \sigma \left[ -(\beta \hat{q})^{-1} \log \text{ran}(0, 1) \right]$  (see Eq. (42))
if  $|x_{\text{ev}}| > n + 1$ :  $x_{\text{ev}} \leftarrow \sigma(n + 1)$ 
else if  $\text{ran}(0, \hat{q}) < \hat{q}^{(2)}$ :
   $\left\{ \begin{array}{l} \text{if } \text{ran}(0, 1) < |x_{\text{ev}}|/\hat{q}^{(2)}: \tilde{\sigma} = -\sigma \end{array} \right.$ 
else:
   $\left\{ \begin{array}{l} \text{if } \text{ran}(0, 1) < |x_{\text{ev}}|^3/\hat{q}^{(4)}: \tilde{\sigma} = -\sigma \end{array} \right.$ 
 $t_{\text{ev}} \leftarrow t + |x_{\text{ev}} - x|$ 
for  $t^* = \text{int}(t) + 1, \dots, \text{int}(t_{\text{ev}})$ :
   $\left\{ \begin{array}{l} \text{print } x + \sigma(t^* - t) \quad (\text{equal-time samples}) \end{array} \right.$ 
 $x \leftarrow x_{\text{ev}}; \sigma \leftarrow \tilde{\sigma}; t \leftarrow t_{\text{ev}}$  ("zig-zag")
output  $\{x, \sigma\}, t$ 

```

**Algorithm 12: bounded-factor-zig-zag(patch).** Patch of Alg. 11 illustrating the bundling of two factors into a single candidate event.

## VI. CONCLUSION

In this paper, we have introduced to a number of modern developments in Monte Carlo sampling that go much beyond direct sampling and the Metropolis algorithm. New Monte Carlo algorithms build on notions such as factorization, non-reversibility and thinning. They increasingly find applications in physics and other sciences. The severely stripped-down one-dimensional anharmonic oscillator has hopefully allowed us to lay bare the foundations of these non-trivial theoretical developments. In a first step, we have concentrated on the correctness of the sampling algorithms. Questions of efficiency will be the subject of the companion paper [2].

## ACKNOWLEDGMENTS

We thank K. J. Wiese for helpful discussions. We thank the mathematical research institute MATRIX in Australia where part of this research was performed.

## Appendix A: Mathematical details

In this appendix, we present some mathematical details that, for the sake of conciseness, were omitted in the main text.

As stated in Eq. (6), the period of the isolated anharmonic oscillator at energy  $E$  is

$$\tau(E) = 4\sqrt{\frac{2}{1 + \sqrt{1 + 4E}}} K\left(\frac{1 - \sqrt{1 + 4E}}{1 + \sqrt{1 + 4E}}\right), \quad (\text{A1})$$

where  $K$  is the complete elliptic integral of the first kind. This non-trivial integral follows from the theory of elliptic functions (see e.g. [16, Ch. 19] for a discussion on the subject). It can be obtained indirectly using the `Integrate` function of the Mathematica software, as illustrated in a Mathematica notebook file made available in the software package (see App. B). For  $E \rightarrow 0$ , the amplitude  $x_{\max}$  of the oscillation is small. Consequently, the anharmonic potential  $U_{24}(x)$  of Eq. (1) can be safely replaced with the harmonic one in this regime:

$$U_{24}(x) \sim U_2(x) = x^2/2 \quad \text{for } x_{\max} \rightarrow 0. \quad (\text{A2})$$

Indeed, expanding  $\tau(E)$  in Eq. (A1) about  $E = 0$ , we obtain

$$\tau(E) = 2\pi - \frac{3\pi}{2}E + \mathcal{O}(E^2).$$

(see App. B for a Mathematica notebook file using the `Series` function).

For small  $E$ , the period of the anharmonic oscillator coincides with that of the harmonic one,  $\tau = 2\pi$ , since the quartic term in the potential is negligible for  $|x| \ll 1$ . On the other hand, for large  $E$ , the quartic term dominates:

$$U_{24}(x) \sim U_4(x) = x^4/4 \quad \text{for } x_{\max} \gg 0.$$

In this case, expanding  $\tau$  for large  $E$ , we have

$$\tau(E) = \frac{\sqrt{\pi}\Gamma(1/4)}{\Gamma(3/4)}E^{-1/4} + \mathcal{O}(E^{-3/4}),$$

where  $\Gamma$  denotes the Euler gamma function (see again App. B for the corresponding Mathematica notebook file). The dominant term of the above expression coincides with the period of the quartic oscillator, computed using the equivalent of Eq. (6), with amplitude  $x_{\max} = (4E)^{1/4}$ .

Finally, the partition function  $Z(\beta)$  of the harmonic oscillator in Eq. (13) can be easily computed by means of the Mathematica `Integrate` function.

## Appendix B: Computer programs, Mathematica notebook files

The present paper is accompanied by the `MCMCNutshell` software package, which is published

as an open-source project under the GNU GPLv3 license. `MCMCNutshell` is available on GitHub as part of the `JeLLyFysh` organization [17]. The package contains Python implementations for  $\beta = 1$  of the algorithms that were discussed here and that were used to produce the results of Table III. It also contains the Mathematica Notebook files discussed in App. A.

## Appendix C: Numerical tests

Except for Alg. 0 (`isolated-dynamics`), the eleven Monte Carlo algorithms and one molecular-dynamics algorithm all sample the Boltzmann distribution  $\pi_{24}$  of Eq. (2). To check the correctness of our implementations, we fixed an arbitrary non-zero value of  $\bar{x} = 0.63$  for  $\beta = 1$ , computed for each algorithm the empirical probability with which the samples  $x$  satisfy  $x < \bar{x}$ , and compared it with the exact result:

$$\mathbb{P}(x < 0.63) = Z^{-1} \int_{-\infty}^{0.63} \pi_{24}(x') dx' = 0.8030245. \quad (\text{C1})$$

Single-standard-deviation error bars were obtained from the bunching method [1, Sec. 1.3.5], except for Alg. 2 (`direct-sampling`), where we performed a standard Gaussian analysis. For all twelve algorithms, results are consistent with Eq. (C1) within three standard deviations (see Table III).

Algorithm	$\mathbb{P}(x < 0.63)$
1 thermostat-dynamics	0.8038 $\pm$ 0.0025
2 direct-sampling	0.8029 $\pm$ 0.0001
3 metropolis	0.8029 $\pm$ 0.0026
4 factor-metropolis	0.8004 $\pm$ 0.0035
5 factor-metropolis(patch)	0.8029 $\pm$ 0.0015
6 lifted-metropolis	0.8033 $\pm$ 0.0003
7 zig-zag	0.80292 $\pm$ 0.00009
8 factor-zig-zag	0.8030 $\pm$ 0.0001
9 bounded-lifted	0.8036 $\pm$ 0.0004
10 bounded-zig-zag	0.80297 $\pm$ 0.00009
11 bounded-factor-zig-zag	0.80297 $\pm$ 0.00007
12 bounded-factor-zig-zag(patch)	0.8029 $\pm$ 0.0001

**TABLE III:** Estimated probability  $\mathbb{P}(x < 0.63)$  for the anharmonic oscillator computed by the algorithms discussed in this paper (single- $\sigma$  error bars).

- 
- [1] W. Krauth, *Statistical Mechanics: Algorithms and Computations* (Oxford University Press, 2006).
- [2] G. Tartero, S. Vionnet, and W. Krauth, Fast sampling of Lennard-Jones systems without cutoffs, manuscript in preparation.
- [3] M. H. A. Davis, Piecewise-Deterministic Markov Processes: A General Class of Non-Diffusion Stochastic Models, *J. R. Stat. Soc. Series B Stat. Methodol.* **46**, 353 (1984).
- [4] L. Landau and E. Lifshitz, *Mechanics: Volume 1*, vol. 1 (Elsevier Science, 1982).
- [5] B. Li, Y. Nishikawa, P. Höllmer, L. Carillo, A. C. Maggs, and W. Krauth, Hard-disk pressure computations—a historic perspective, *The Journal of Chemical Physics* **157**, 234111 (2022).
- [6] M. Michel, S. C. Kapfer, and W. Krauth, Generalized event-chain Monte Carlo: Constructing rejection-free global-balance algorithms from infinitesimal steps, *J. Chem. Phys.* **140**, 054116 (2014).
- [7] P. Diaconis, S. Holmes, and R. M. Neal, Analysis of a nonreversible Markov chain sampler, *Ann. Appl. Probab.* **10**, 726 (2000).
- [8] F. Chen, L. Lovász, and I. Pak, Lifting Markov Chains to Speed up Mixing, Proceedings of the 17th Annual ACM Symposium on Theory of Computing , 275 (1999).
- [9] J. Bierkens, P. Fearnhead, and G. Roberts, The Zig-Zag process and super-efficient sampling for Bayesian analysis of big data, *Ann. Stat.* **47**, 1288 (2019).
- [10] D. A. Levin, Y. Peres, and E. L. Wilmer, *Markov Chains and Mixing Times* (American Mathematical Society, 2008).
- [11] W. Krauth, Event-Chain Monte Carlo: Foundations, Applications, and Prospects, *Front. Phys.* **9**, 229 (2021).
- [12] E. A. J. F. Peters and G. de With, Rejection-free Monte Carlo sampling for general potentials, *Phys. Rev. E* **85**, 026703 (2012).
- [13] P. A. W. Lewis and G. S. Shedler, Simulation of non-homogeneous Poisson processes by thinning, *Naval Research Logistics Quarterly* **26**, 403 (1979).
- [14] S. C. Kapfer and W. Krauth, Cell-veto Monte Carlo algorithm for long-range systems, *Phys. Rev. E* **94**, 031302 (2016).
- [15] A. J. Walker, An Efficient Method for Generating Discrete Random Variables with General Distributions, *ACM Trans. Math. Softw.* **3**, 253 (1977).
- [16] NIST Digital Library of Mathematical Functions, <http://dlmf.nist.gov/>, edited by F. W. J. Olver, A. B. Olde Daalhuis, D. W. Lozier, B. I. Schneider, R. F. Boisvert, C. W. Clark, B. R. Miller, B. V. Saunders, H. S. Cohl, and M. A. McClain.
- [17] The url of the repository is <https://github.com/jellyfysh/MCMCNutshell>.